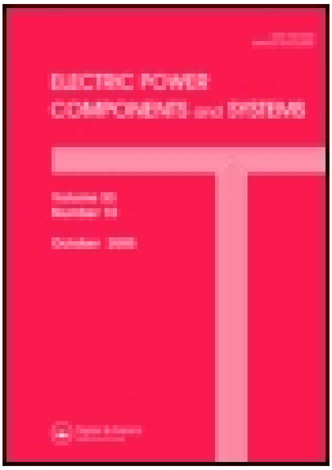

Electric Power Components and Systems
Publication details, including instructions for authors and subscription information:
http://www.tandfonline.com/loi/uemp20

A Deadbeat Active and Reactive Power Control for Doubly Fed Induction Generator

A. J. Sguarezi Filho [a] & E. Ruppert [a]
[a] FEEC-DSCE, University of Campinas, Campinas, SP, Brazil
Published online: 22 Mar 2010.

Electric Power Components and Systems, 38:592–602, 2010

ISSN: 1532-5008 print/1532-5016 online
DOI: 10.1080/15325000903376966

A Deadbeat Active and Reactive Power Control for Doubly Fed Induction Generator

A. J. SGUAREZI FILHO[1] and E. RUPPERT[1]

[1]FEEC-DSCE, University of Campinas, Campinas, SP, Brazil

Abstract *This article proposes a power control scheme for doubly fed induction generator for variable speed wind power generation. This scheme uses a deadbeat control loop. The algorithm of the deadbeat calculates at each sample period the voltage vector to be supplied to the rotor in order to guarantee that the active and reactive power reach their desired reference values. The robustness of the controller against rotor resistance variation was evaluated. Simulations results are carried out for validation of the digital controller operation.*

Keywords doubly fed induction generator, power control, deadbeat control, wind energy, variable-speed constant frequency applications

1. Introduction

Renewable energy systems, especially wind energy, have attracted interest due to the increasing concern about CO_2 emissions. The wind energy systems using a doubly fed induction generator (DFIG) have some advantages due to variable-speed operation and four-quadrant active and reactive power capabilities compared with fixed-speed induction squirrel-cage generators presented in [1, 2].

The control of DFIG wind turbine systems is traditionally based on either stator-flux-oriented [3] or stator-voltage-oriented [4] vector control. The scheme decouples the rotor current into active and reactive power components. Control of the active and reactive powers is achieved with a rotor current controller. Some investigations used stator-flux-oriented proportional-integral (PI) controllers, which generate reference currents from active and reactive power errors to the inverter, or cascade PI controllers, which generate a rotor voltage [5, 6]. The problem in the use of a PI controller is the tuning of the gains and the cross-coupling on the DFIG terms in the whole operating range. An interesting method to solve these problems has been presented in [7–9].

Some investigations using the predictive functional controller [10] and internal mode controller [11, 12] have shown satisfactory power response when compared with the power response of PI, but it is hard to implement due to the predictive functional controller and internal mode controller formulation. Another possibility to DFIG power control can be made by using fuzzy logic [13, 14]. At each sample interval, the controllers calculate the voltage rotor to be supplied to the DFIG to guarantee that active and reactive power reach their desired reference values. These strategies have satisfactory power response,

Received 8 June 2009; accepted 30 September 2009.
Address correspondence to Mr. Alfeu J. Sguarezi Filho, FEEC-DSCE, University of Campinas, CP 6101, CEP 13083-852, Campinas, SP, Brazil. E-mail: sguarezi@dsce.fee.unicamp.br

although it involves relatively complex transformation of voltages, currents, and control outputs among the stationary, rotor, and synchronous reference frames.

A direct power control was proposed based on the principles of direct torque control strategy in [15–17]. This scheme calculates the required rotor controlling voltage within each sampling period directly based on the estimated stator flux, active and reactive powers, and their errors. Meanwhile, a constant switching frequency was achieved by the space vector modulation (SVM) technique. However, this method still encounters some problems such as over-current under grid voltage sags.

This article proposes a deadbeat power control scheme for a DFIG. The deadbeat power control aims the active and reactive power control using the DFIG equations in a synchronous coordinate system. The deadbeat controller calculates the rotor voltages required to guarantee that active and reactive power reach their desired reference values at each sample period. Simulation results are presented for validation the proposed controller.

2. Machine Model and Vector Control

The DFIG model in synchronous reference frame is given by [18]

$$\vec{v}_{1dq} = R_1\vec{i}_{1dq} + \frac{d\vec{\lambda}_{1dq}}{dt} + j\omega_1\vec{\lambda}_{1dq}, \tag{1}$$

$$\vec{v}_{2dq} = R_2\vec{i}_{2dq} + \frac{d\vec{\lambda}_{2dq}}{dt} + j(\omega_1 - NP\omega_{mec})\vec{\lambda}_{2dq}; \tag{2}$$

the relationship between fluxes and currents

$$\vec{\lambda}_{1dq} = L_1\vec{i}_{1dq} + L_M\vec{i}_{2dq}, \tag{3}$$

$$\vec{\lambda}_{2dq} = L_M\vec{i}_{1dq} + L_2\vec{i}_{2dq}, \tag{4}$$

and generator active and reactive power are

$$P = \frac{3}{2}(v_{1d}i_{1d} + v_{1q}i_{1q}), \tag{5}$$

$$Q = \frac{3}{2}(v_{1q}i_{1d} - v_{1d}i_{1q}). \tag{6}$$

where

subscripts "1" and "2" represent the stator and rotor parameters, respectively;
ω_1 is the synchronous speed;
ω_{mec} is the machine speed;
R_1 and R_2 are the estator and rotor windings per phase electrical resistance;
L_1, L_2, and L_m are the proper and mutual inductances of the stator and rotor windings;
$\vec{v}$ is the voltage vector; and
NP is the machine number of pair of poles.

DFIG power control aims at independent stator active P and reactive Q power control by means of a rotor current regulation. For this purpose, P and Q are represented as functions of each individual rotor current. Using stator-flux-oriented control, the decoupled dq-axis in Eq. (3) becomes

$$i_{1d} = \frac{\lambda_1}{L_1} - \frac{L_M}{L_1} i_{2d}, \tag{7}$$

$$i_{1q} = -\frac{L_M}{L_1} i_{2q}, \tag{8}$$

where λ_1 is the magnitude of the stator flux space vector $\vec{\lambda}_{1dq}$.

The active (Eq. (5)) and reactive (Eq. (6)) powers can be calculated by using Eqs. (7) and (8) as

$$P = -\frac{3}{2} v_1 \frac{L_M}{L_1} i_{2q}, \tag{9}$$

$$Q = \frac{3}{2} v_1 \left(\frac{\lambda_1}{L_1} - \frac{L_M}{L_1} i_{2d} \right), \tag{10}$$

where $v_1 = v_{1q}$.

Thus, rotor currents will reflect in stator currents and on stator active and reactive power. Consequently, this principle can be used on stator active and reactive power control by using current control on the rotor side in the DFIG with the stator connected to the grid.

2.1. Rotor-side Equations

The control of rotor currents in Eqs. (9) and (10) allows DFIG power control. By the rotor voltage in Eq. (2) in the synchronous referential frame using the stator flux position, Equations (7) and (8) become

$$\vec{v}_{2dq} = (R_2 + jL_2\omega_{sl})\vec{i}_{2dq} + jL_m\omega_{sl}\vec{i}_{1dq} + \left(L_2 - \frac{L_M^2}{L_1} \right) \frac{d\vec{i}_{2dq}}{dt}, \tag{11}$$

where $\omega_{sl} = \omega_1 - NP\omega_{mec}$.

In space-state form, Eq. (11) becomes

$$\dot{\bar{i}}_2 = H\bar{i}_2 + K\bar{v}_2 + L\bar{i}_1, \tag{12}$$

$$\begin{bmatrix} \frac{di_{2d}}{dt} \\ \frac{di_{2q}}{dt} \end{bmatrix} = \begin{bmatrix} \frac{-R_2}{\sigma L_2} & \frac{\omega_{sl}}{\sigma} \\ \frac{-\omega_{sl}}{\sigma} & \frac{-R_2}{\sigma L_2} \end{bmatrix} \begin{bmatrix} i_{2d} \\ i_{2q} \end{bmatrix} + \begin{bmatrix} \frac{1}{\sigma L_2} & 0 \\ 0 & \frac{1}{\sigma L_2} \end{bmatrix} \begin{bmatrix} v_{2d} \\ v_{2q} \end{bmatrix} + \begin{bmatrix} 0 & \frac{\omega_{sl} L_M}{\sigma L_2} \\ \frac{-\omega_{sl} L_M}{\sigma L_2} & 0 \end{bmatrix} \begin{bmatrix} i_{1d} \\ i_{1q} \end{bmatrix}, \tag{13}$$

where $\sigma = 1 - \frac{L_M^2}{L_1 L_2}$. Henceforth, it will be assumed that the mechanical time constant is much greater then the electrical time constants. Thus, $\omega_{mec} = constant$ is a valid approximation [19, 20].

3. The Deadbeat Control

The deadbeat control is a digital control technique that allows the calculation of the required input $\bar{u}(k)$, guaranteeing that the output $\bar{x}(k)$ will reach its desired reference values in only one sample interval, using a discrete equation of the continuous linear system [21, 22].

A linear continuous system is represented by

$$\dot{\bar{x}} = A\bar{x} + B\bar{u} + G\bar{w},$$
$$\bar{y} = C\bar{x}, \tag{14}$$

where $\bar{w}$ denotes the perturbation vector and A, C, B, and G are $n \times n$ matrices. In this article, $C = I$, where I is the identity matrix.

Equation (14) can be discretized, considering T as the sampling period and k as the sampling time, by using a zero-order hold (ZOH) with no delay as

$$\bar{x}(k+1) = A_d\bar{x}(k) + B_d\bar{u}(k) + G_d\bar{w}(k), \tag{15}$$

where

$$A_d = e^{AT} \cong I + AT,$$
$$B_d = \int_0^{\tau} e^{AT} B\, d\tau \cong BT, \tag{16}$$
$$G_d = \int_0^{\tau} e^{AT} G\, d\tau \cong GT.$$

The input calculation to guarantee a null steady-state error is given by

$$\bar{u}(k) = F(\bar{x}_{ref} - \bar{x}), \tag{17}$$

where $\bar{x}_{ref}$ is the reference vector, and F is the matrix gain.

Substituting Eq. (17) into Eq. (15) and making $\bar{x}_{ref} = \bar{x}(k+1)$, the input that guarantees a null steady-state error is given by

$$\bar{u}(k) = B_d^{-1} A_d \left[A_d^{-1}\bar{x}_{ref} - \bar{x}(k) - A_d^{-1} G_d \bar{w}(k)\right]. \tag{18}$$

3.1. Power Control

The control scheme uses a deadbeat controller to obtain rotor voltages that should be applied on the generator in order to guarantee that the active and reactive powers reach their desired reference values in only one sample interval. It has the same time of the pulse width modulation (PWM) modulator. The converter that is connected to the grid controls the voltage of the link DC, and it can be controlled by using the current control presented in [23]. The deadbeat power control block diagram is shown in Figure 1.

The rotor equation (Eq. (13)) can be rewritten as a discrete equation using Eq. (15) and making $\bar{x} = \bar{i}_2$, $A = H$, $B = K$, $\bar{u} = \bar{v}_2$, $G = L$, and $\bar{w} = \bar{i}_1$. It is given

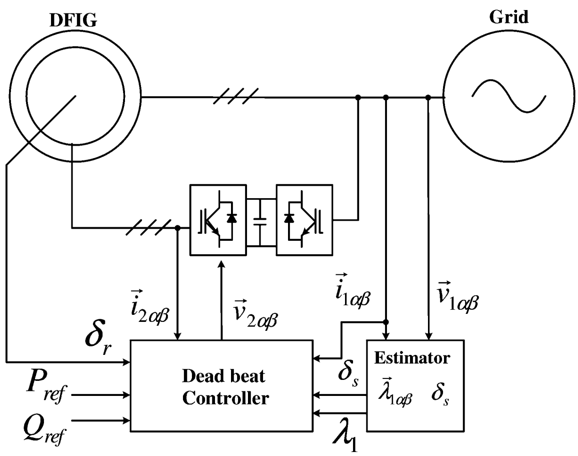

Figure 1. Deadbeat power control block diagram.

by Eq. (19):

$$\begin{bmatrix} i_{2d}(k+1) \\ i_{2q}(k+1) \end{bmatrix} = \begin{bmatrix} 1-\dfrac{R_2T}{\sigma L_2} & \dfrac{\omega_{sl}T}{\sigma} \\ \dfrac{-\omega_{sl}T}{\sigma} & 1-\dfrac{R_2T}{\sigma L_2} \end{bmatrix} \begin{bmatrix} i_{2d}(k) \\ i_{2q}(k) \end{bmatrix} + \begin{bmatrix} \dfrac{T}{\sigma L_2} & 0 \\ 0 & \dfrac{T}{\sigma L_2} \end{bmatrix} \begin{bmatrix} v_{2d}(k) \\ v_{2q}(k) \end{bmatrix} + \begin{bmatrix} 0 & \dfrac{\omega_{sl}L_MT}{\sigma L_2} \\ \dfrac{-\omega_{sl}L_MT}{\sigma L_2} & 0 \end{bmatrix} \begin{bmatrix} i_{1d}(k) \\ i_{1q}(k) \end{bmatrix}. \tag{19}$$

The rotor voltage, which is calculated to guarantee the null steady-state error by using Eqs. (18) and (19), is given by

$$v_{2d}(k) = \sigma L_2 \frac{i_{2d}(k+1) - i_{2d}(k)}{T} + R_2 i_{2d}(k) - L_2\omega_{sl} i_{2q}(k) - L_M\omega_{sl} i_{1q}(k), \tag{20}$$

$$v_{2q}(k) = \sigma L_2 \frac{i_{2q}(k+1) - i_{2q}(k)}{T} + R_2 i_{2q}(k) + L_2\omega_{sl} i_{2d}(k) + L_M\omega_{sl} i_{1d}(k). \tag{21}$$

For the active power control (from Eq. (9)), the rotor current reference is given by

$$i_{2q}(k+1) = i_{2q_{ref}} = -\frac{2P_{ref}L_1}{3v_1L_M}, \tag{22}$$

and for the reactive power control (from Eq. (10)), it is

$$i_{2d}(k+1) = i_{2d_{ref}} = -\frac{2Q_{ref}L_1}{3v_1L_M} + \frac{\lambda_1}{L_M}. \tag{23}$$

Thus, if the d- and q-axis voltage components, calculated according to Eqs. (20), (21), (22), and (23), are applied to the generator, then the active and reactive power convergence to their respective commanded values will occur in one sampling interval. The desired rotor voltage in the rotor reference frame ($\delta_s - \delta_r$) generates switching signals for the rotor side using SVM.

Stator currents and voltages and rotor speed and currents are measured to stator flux position δ_s, magnitude λ_1, synchronous frequency ω_1, and slip frequency ω_{sl} for estimation.

3.2. Estimation

For deadbeat power control, as shown in Eqs. (20) and (21), one must calculate the active and reactive power values, their errors, the stator flux magnitude and position, the slip speed, and synchronous frequency. The stator flux $\vec{\lambda}_{1\alpha\beta}$ estimation in the stationary reference frame is given by

$$\vec{\lambda}_{1\alpha\beta} = \int (\vec{v}_{1\alpha\beta} - R_1 \vec{i}_{1\alpha\beta}) dt, \tag{24}$$

and the stator flux position by using Eq. (24) as

$$\delta_s = \arctan\left(\frac{\lambda_{1\beta}}{\lambda_{1\alpha}}\right). \tag{25}$$

The synchronous speed ω_1 estimation is given by

$$\omega_1 = \frac{d\delta_s}{dt} = \frac{(v_{1\beta} - R_1 i_{1\beta})\lambda_{1\alpha} - (v_{1\alpha} - R_1 i_{1\alpha})\lambda_{1\beta}}{(\lambda_{1\alpha})^2 + (\lambda_{1\beta})^2}, \tag{26}$$

and the slip speed estimation by using the rotor speed and synchronous speed is

$$\omega_{sl} = \omega_1 - NP\omega_{mec}. \tag{27}$$

The angle between stator and rotor flux is given by

$$\delta_s - \delta_r = \int \omega_{sl} dt. \tag{28}$$

3.3. Simulation Results

The simulation of the proposed digital control strategy was performed with the MATLAB/ SimPowerSystems® package (The MathWorks, Natick, Massachusetts, USA). The digital power control strategy has a $T = 0.5\ 10^{-4} s$, and the DFIG parameters are shown in the appendix. Figure 1 shows the schematic of the implemented system. For power factor (PF) control, the reactive power reference is given by

$$Q_{ref} = P_{ref} \frac{\sqrt{1 - PF^2}}{PF}.$$

Initial studies with various active and reactive power steps (constant rotor speed of 226.6 rad/s) were carried out to test the dynamic response of the proposed power control strategy, and it is shown in Figure 2(a). The initial active power and PF references were −60 kW and a PF of +0.85. The active power and PF references were step changed from −60 to −100 kW and from a PF of 0.85 to −0.85 at 1.75 sec; the power references

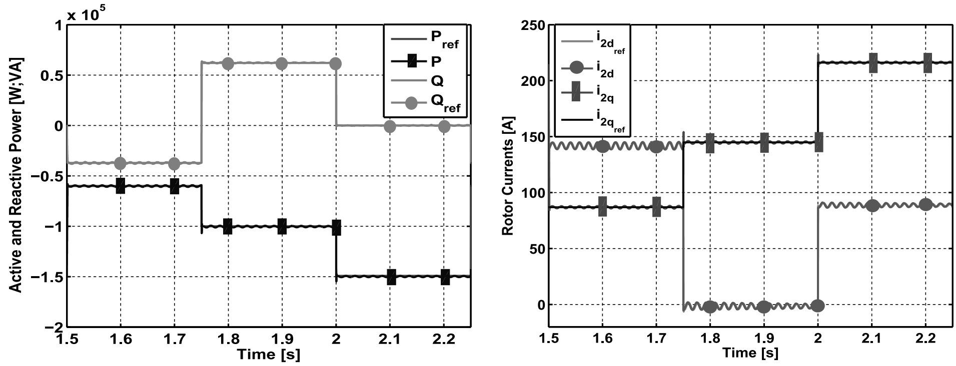

(a) (b)

Figure 2. Response of step tests for active and reactive power and rotor currents in super-synchronous operation: (a) response of step of active and reactive power and (b) response of step of rotor currents in synchronous referential.

were step changed again from −100 to −149.2 kW and from a PF of −0.85 to 1 at 2 sec, respectively. The rotor currents in the synchronous referential is shown in Figure 2(b), and the rotor and stator currents in the stationary referential are shown in Figure 3. The dynamic response of both the active and reactive powers is a few milliseconds; there is no overshoot of either stator/rotor or active/reactive powers, and the satisfactory performance and robustness of the controller can be seen.

Studies with various power steps and rotor speed were carried out to further test the proposed power control strategy. During the period 1.75–2.09 sec, the rotor speed increased from 151.1 to 226.6 rad/s. Figure 4(a) shows the results step reference tests of active and reactive power. The power steps, *i.e.*, active power and PF references, were changed from −60 to −100 kW and from a PF of 0.85 to −0.85 at 1.75 sec. The rotor currents in the synchronous referential are shown in Figure 4(b), the rotor speed and rotor and stator currents in the stationary referential are shown in Figure 5, and the voltage of the capacitor is presented in Figure 6. The satisfactory performance and robustness of the controller can be seen due to the fact that the active and reactive powers reach their desired reference values when the rotor speed varies.

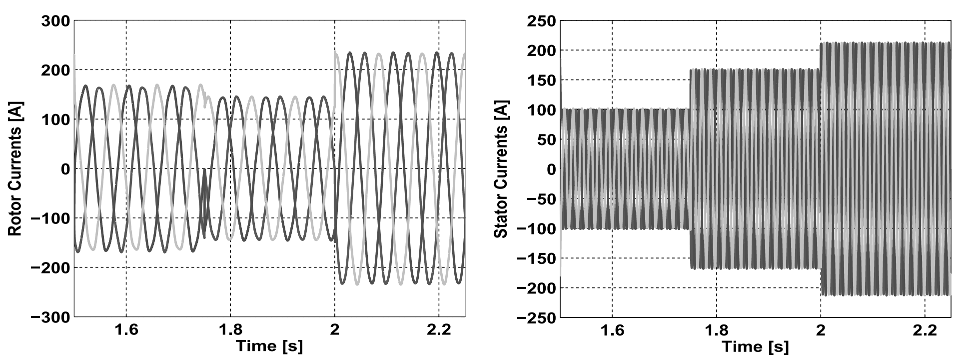

(a) (b)

Figure 3. Stator and rotor currents: (a) rotor currents and (b) stator currents.

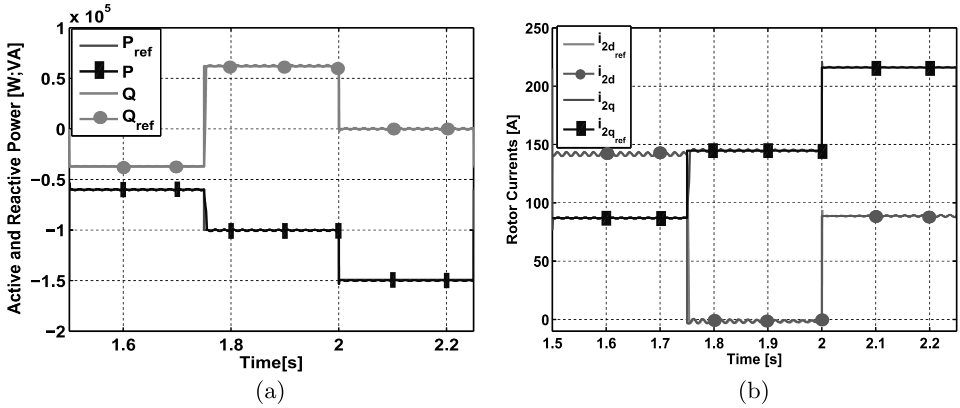

Figure 4. Response of step tests for active and reactive power and rotor currents with several speed operations: (a) response of step of active and reactive power and (b) response of step of rotor currents in synchronous referential.

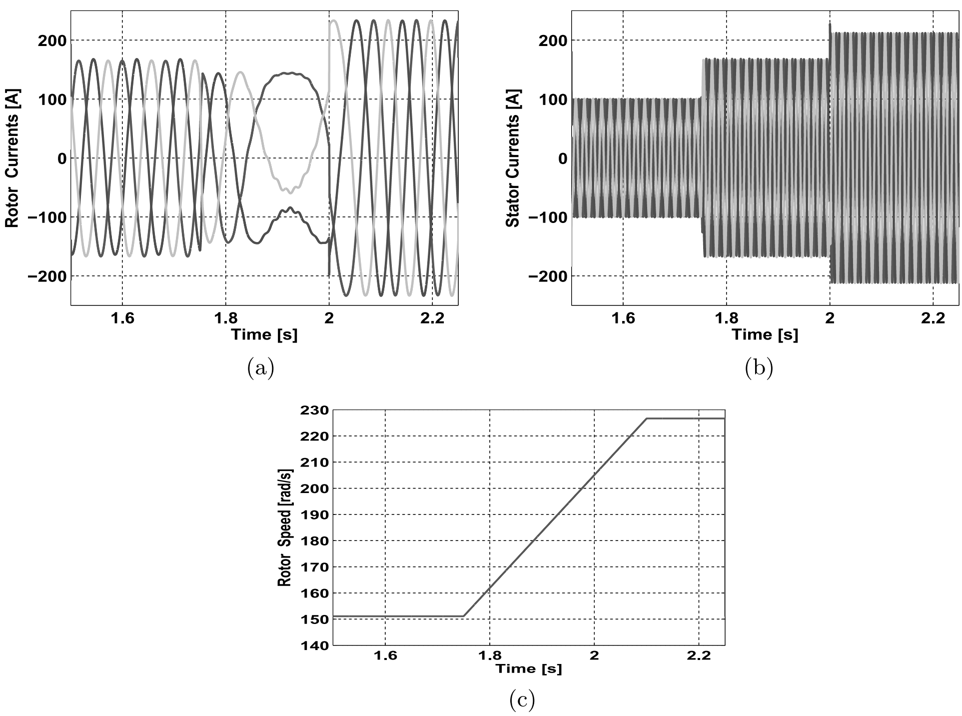

Figure 5. Stator and rotor currents and rotor speed: (a) rotor currents, (b) stator currents, and (c) rotor speed.

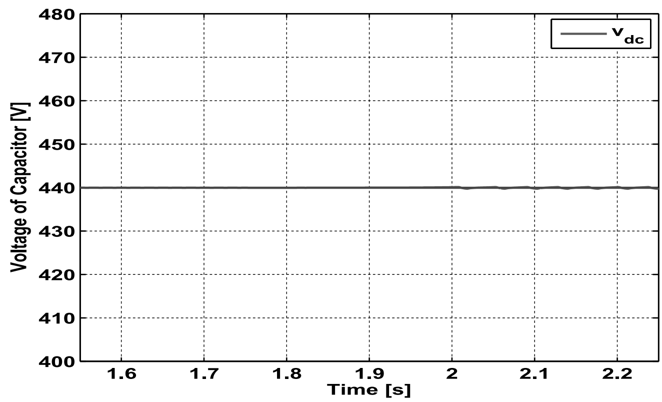

Figure 6. DC link voltage.

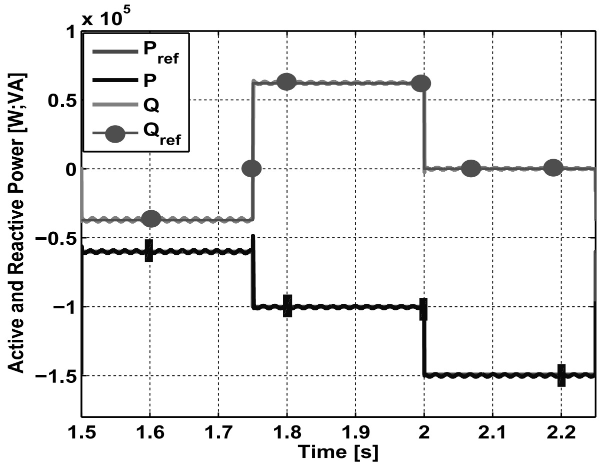

Figure 7. Response of step tests for active and reactive power with parameter variations.

To test the impact of the parameter variations on the system performance, the rotor resistance R_2 of the DFIG was increased by 20%. The same tests of step reference of active and reactive powers with rotor speed variation and with the rotor resistance variation are shown in Figure 7. Comparing Figures 4(a) and 7, there is hardly any difference, and even with such rotor resistance errors, the system maintains satisfactory performance under both steady-state and transient conditions.

4. Conclusion

This article has presented a power control scheme for a DFIG using a deadbeat control loop. The controller uses DFIG-discretized equations to calculate the required rotor voltages at each sample period for the active and the reactive power values to reach their desired reference values. Thus, the deadbeat controller do not need to tune gains, as do PI controllers [5, 9]. This strategy has a similar power response to the direct power control presented in [16, 17], and the constant switching frequency overcomes the drawbacks of conventional direct power control [15, 16].

The impact of rotor resistance variation was also analyzed on the deadbeat controller, and it was found to be satisfactory due to the fact that the system maintains satisfactory performance under both steady-state and transient conditions. The power control scheme helps the protection of the rotor-side converter because there is no overshoot in the rotor current. The simulations confirm the effectiveness and the robustness of the power controller during several operating conditions of machine speed.

References

1. Simões, M. G., and Farret, F. A., *Renewable Energy Systems with Induction Generators*, Boca Raton, FL: CRC Press, 2004.
2. Datta, R., and Rangathan, V. T., "Variable-speed wind power generation using doubly fed wound rotor induction machine—a comparison with alternative schemes," *IEEE Trans. Energy Conversion*, Vol. 17, No. 3, pp. 414–421, September 2002.
3. Chowdhury, B. H., and Chellapilla, S., "Double-fed induction generation control for variable speed wind power generation," *Elect. Power Syst. Res.*, Vol. 76, pp. 786–800, 2006.
4. Hopfensperger, B., Atkinson, D. J., and Lakin, R., "Stator-flux-oriented control of a doubly-fed induction machine with and without position encoder," *IEE Proc. Elect. Power Appl.*, Vol. 147, No. 4, pp. 241–250, April 2000.
5. Tapia, A., Tapia, G., Ostolaza, J. X., and Sáenz, J. R., "Modeling and control of a wind turbine driven doubly fed induction generator," *IEEE Trans. Energy Conversion*, Vol. 18, No. 2, pp. 194–204, June 2003.
6. Bim, E., and Jacomini, R. V., "Controle do fator de potência de um gerador de indução duplamente alimentado conectado á rede-operação com escorregamento positivo," *Congresso Brasileiro de Automática (CBA/2008)*, Juiz de Fora, MG-Brazil, September 2008.
7. da Costa, J. P., Marques, J., Gründling, H. A., and Pinheiro, H., "Dynamic behavior of the doubly-fed induction generator in stator flux vector reference frame," *Eletrônica de Potência*, Vol. 13, No. 1, pp. 33–42, March 2006.
8. de Oliveira, R. G., da Silva, J. L., and Silva, S. R., "Development of a new reactive power control strategy in doubly-fed induction generators for wind turbines," *Eletrônica Potência*, Vol. 13, No. 4, pp. 277–284, 2008.
9. Poitiers, F., Bouaouiche, T., and Machmoum, M., "Advanced control of a doubly-fed induction generator for wind energy conversion," *Elect. Power Syst. Res.*, Vol. 79, pp. 1085–1096, 2009.
10. Xin-fang, Z., Da-ping, X., and Yi-bing, L., "Predictive functional control of a doubly fed induction generator for variable speed wind turbines," *IEEE World Congress on Intelligent Control and Automation*, Hangzhou, China, 15–19 June 2004.
11. Morren, J., Sjoerd, M., and de Haan, W. H., "Ridethrough of wind turbines with doubly-fed induction generator during a voltage dip," *IEEE Trans. Energy Conversion*, Vol. 20, No. 2, pp. 435–441, June 2005.
12. Guo, J., Cai, X., and Gong, Y., "Decoupled control of active and reactive power for a grid-connected doubly-fed induction generator," *Third International Conference on Electric Utility Deregulation and Restructuring and Power Technologies (DRPT 2008)*, pp. 2620–2625, Nanjing, China, 6–9 April 2008.
13. Vieria, J. P. A., Nunes, M. V. A., Bezerra, U. H., and do Nascimento, A. C., "Controladores fuzzy aplicados ao conversor de geradores de indução duplamente excitados em sistemas eólicos integrados a sistemas de potência," *Revista Controle Automação*, Vol. 18, No. 1, pp. 115–126, January–March 2007.
14. Yao, X., Jing, Y., and Xing, Z., "Direct torque control of a doubly-fed wind generator based on grey-fuzzy logic," *International Conference on Mechatronics and Automation (ICMA 2007)*, pp. 3587–3592, Harbin, China, 5–8 August 2007.
15. Datta, R., and Ranganathan, V. T., "Direct power control of grid-connected wound rotor induction machine without rotor position sensors," *IEEE Trans. Power Electron.*, Vol. 16, No. 3, pp. 390–399, May 2001.

16. Xu, L., and Cartwright, P., “Direct active and reactive power control of DFIG for wind energy generation,” *IEEE Trans. Energy Conversion*, Vol. 21, No. 3, pp. 750–758, September 2006.
17. Zhi, D., and Xu, L., “Direct power control of DFIG with constant switching frequency and improved transient performance,” *IEEE Trans. Energy Conversion*, Vol. 22, No. 1, pp. 110–118, March 2007.
18. Leonhard, W., *Control of Electrical Drives*, Berlin, Heidelberg, New York, Tokyo: Springer-Verlag, 1985.
19. Holtz, J., Quan, J., Pontt, J., Rodríguez, J., Newman, P., and Miranda, H., “Design of fast and robust current regulators for high-power drives based on complex state variables,” *IEEE Trans. Industry Appl.*, Vol. 40, pp. 1388–1397, September/October 2004.
20. Filho, A. J. S., and Filho, E. R., “The complex controller applied to the induction motor control,” *IEEE APEC*, Vol. 40, pp. 1791–1795, February 2008.
21. Franklin, G. F., Powel, J. D., and Workman, M. L., *Digital Control of Dynamic Systems*, USA: Addison-Wesley Publishing Company, 1994.
22. Filho, A. J. S., de Oliveira Filho, M., and Filho, E. R., “A digital active and reactive power control for doubly-fed induction generetator,” *IEEE Power Electronics Specialists Conference (PESC 2008)*, pp. 2718–2722, Rhodes, Greece, June 2008.
23. Rodríguez, J. R., Dixon, J. W., Espinoza, J. R., Pontt, J., and Lezana, P., “PWM regenerative rectifiers: State of the art,” *IEEE Trans. Industry Electron.*, Vol. 52, No. 1, pp. 5–22, February 2005.

Appendix

The DFIG parameters are as follows:

$R_1 = 0.02475\ \Omega$
$R_2 = 0.0133\ \Omega$
$L_m = 0.01425$ H
$L_{l1} = 0.000284$ H
$L_{l2} = 0.000284$ H
$J = 2.6$ Kg·m^2
$NP = 2$
$PN = 149.2$ kVA
$V_N = 575$ V